RESEARCH ARTICLE

INTERNATIONAL RESEARCH JOURNAL OF MULTIDISCIPLINARY TECHNOVATION

Asian Research Association

DOI: 10.54392/irjmt25312

Optimized Computer Vision Model for Accurate Polyp Detection in Endoscopic Procedures

T. Swetha Kumari [a,*], R. Vasuki [a]

[a] Department of Biomedical Engineering, Bharath Institute of Higher Education and Research, Chennai, India

* Corresponding Author Email: swetha837@gmail.com

DOI: https://doi.org/10.54392/irjmt25312

Received: 17-02-2025; Revised: 21-04-2025; Accepted: 29-04-2025; Published: 04-05-2025

Abstract: Colorectal Cancer (CRC) is the main reason for cancer-linked morbidity and death globally, and early recognition has an important responsibility in enhancing patient endurance rates. Detecting polyp's precursors to CRC significantly reduces mortality when identified in the early stages. The data is gathered from endoscopic video data from publicly available datasets. The preprocessing pipeline includes Contrast-Limited Adaptive Histogram Equalization (CLAHE) to enhance image contrast, followed by Histogram of Gradients (HOG) for feature extraction. This research introduces a framework for concurrent polyp detection in endoscopic videos utilizing advanced computer vision techniques, specifically the Adaptive Masked Cuttlefish Region Convolve NeuroNet (AMC-RCN). This hybrid model integrates the strengths of Mask Region Convolve NeuroNet (R-CNN) and Adaptive Cuttlefish Optimization (ACFO) to achieve precise and efficient polyp detection. The Mask R-CNN component utilizes Region Proposal Networks (RPN) to accurately locate polyps, generating bounding boxes and pixel-wise segmentation masks. The ACFO algorithm further refines the model by optimizing hyper-parameters, improving segmentation boundaries, and selecting the most relevant features from the endoscopic frames, ensuring optimal performance. The AMC-RCN framework effectively handles small and irregular polyps, ensuring high segmentation (98.02%), precision (97.91), F1-score (96.97%), and recall (97.07%) even in complex and challenging scenarios. The model is evaluated on prominent video datasets, providing a comprehensive set of endoscopic video footage for rigorous testing. The framework demonstrates superior detection accuracy, faster training convergence, and robust performance in clinical applications.

Keywords: Polyp Detection, Endoscopic Videos, Advanced Computer Vision, Adaptive Masked Cuttlefish Region Convolve NeuroNet (AMC-RCN), Colorectal Cancer

1. Introduction

The Gastrointestinal Tract (GT) is the main digestive tract of human beings. It comprises mouth, throat, esophagus, stomach, small and large intestines, and anus. This organ performs various critical activities in the human system, such as absorption, digestion, and evacuation. The GT is divided into two parts, including the lower and upper parts. The upper digestive system includes the mouth, esophagus, stomach, and small intestine, which are responsible for first digestion. The lower GT incorporates the intestines and the abdomen, which are important for absorbing water and eliminating waste [1]. The GI tract is sensitive to several pathologic situations, such as infections and sickness that progress and develop into hazardous tumors. Cancer refers to the uncontrolled development and division of bodily cells. This causes aberrant cell formation and separation in GI tract tissue, resulting in tumors. This is known as a colon tumor. Cancer remains the most frequent and main cause of death globally [2]. GI tract tumors are a substantial subset. Approximately 153,020 people are at risk of developing Colorectal Cancer (CRC), with a projected 52,550 deaths. Early detection of CRC leads to effective treatment options [3]. Regular screening of at-risk populations is necessary to identify early symptoms of cancer, such as polyps. Gastric polyps are irregular developments that protrude from the mucosal surface. Early identification of polyps is crucial for cancer screening and treatment, leading to improved survival rates, less morbidity, and lower costs. In the contemporary world, it presents a significant difficulty. Stomach cancer made up 33% of all instances during the preceding five years, while CRC accounted for 63% [4]. CRC has several stages, with stage IV being the most dangerous and having only a 3% chance of survival. Surprisingly, 95% of patients have overcome the early stage. To effectively treat CRC, precancerous abnormalities must be identified and removed. Finding colon polyps is particularly crucial since they later

progress to CRC. To reduce the fatality rate, it is crucial to actively pursue early detection of CRC. The urgency of taking action highlights the need for forceful and aggressive measures to deal with this issue head-on [5]. Proactive patient monitoring relies heavily on the colonoscopy process since it seeks to identify abnormalities early. This advanced method is especially important for detecting inflammation in the colon and rectum by offering a thorough assessment. Patients are strongly advised to have a colonoscopy by gastroenterologists and endoscopists, who use advanced camera equipment to ensure accuracy [6]. It is crucial to accurately detect polyps, which are abnormal tissue growths in the GT, particularly in the colorectal region, to encourage proactive health management and prevent CRC from progressing to more severe stages. Colorectal polyps are classified into three sizes: tiny (≤ 5mm), medium (6-9mm), and large (≥ 10mm). Larger polyps are typically discovered and removed during standard endoscopic procedures. There are three types of polyps: hyperplastic, adenomatous, and serrated. Adenomatous polyps are more similar to cancer, making them a cause for concern. The risk of a polyp transforming into cancer is proportional to its size and degree of dysplasia [7]. Currently, gastroenterologists use endoscopic methods to manually diagnose polyps. Early diagnosis and removal of polyps are critical for cancer prevention. Regular screening is crucial for those aged 45 and above in healthcare systems. By 2050, the worldwide populace aged 45 and over is expected to achieve 52.5%, up from 43.8% today. Manual CRC screening for a large population is not a practical solution due to operator proficiency affecting accuracy. Research is being performed to build Continuous Ambulatory Peritoneal Dialysis (CAPD) techniques that detect polyps and provide secondary opinions in addition to gastroenterologists. Various disease detection technologies have limitations in precision and speed, especially for real-time detection. Currently, combining AI-based detection systems with existing endoscopic equipment requires additional hardware [8]. However, in the future, these systems will be integrated directly to produce a small disease detection system powered by Artificial Intelligence (AI). AI is at present commonly used to create automated systems for polyp classification, identification, and segmentation. Effective polyp detection algorithms require strong handling of fluctuating polyp imaging. These systems should have low polyp miss rates and provide real-time identification for therapeutic applications. Additionally, they must be able to discriminate between polyps and related structures, such as air bubbles, colon folds, and blood arteries. Efforts to improve accuracy and reduce miss rates for small or miniature polyps continue to be a priority in polyp detection research. New techniques, like enhanced activation functions, transfer learning, data augmentation, and feature optimization, have improved frameworks by addressing the issue of limited training data [9]. Detecting polyps utilizing AI and other detectors has enhanced, but achieving superior accuracy rates while preserving concurrent presentation remains a complexity. Numerous techniques survive for categorizing, distinguishing, and segmenting gastric polyps, according to the literature review. While a huge evolution has been completed, additional effort is required to process and improve current methods for medical procedures. There is currently no one measure to estimate object detection approaches based on accuracy, resource consumption, and speed. A requirement of frequent metrics borders precise assessments among models. The research highlights the significance of improving accuracy and robustness for concurrent polyp detection. Current techniques have diverse degrees of accuracy, and their concurrent relevance presents substantial trouble. Bridging the accuracy-speed gap is significant in assuring these methods' realistic applicability in experimental surroundings. Advancements in methods and algorithms strike an improved stability among precision and concurrent capabilities, opening up novel potential for future research in concurrent polyp recognition [10]. The research objective is to generate a superior concurrent polyp detection framework for endoscopic videos to improve segmentation accuracy, optimize trait selection, and efficiently identify small and irregular polyps. This research aims to improve early CRC detection by Adaptive Masked Cuttlefish Region Convolve Neuronet (AMC-RCN), eventually leading to higher detection accuracy and consistent experimental application.

1.1 Highlights of the Research

CRC remains a main source of cancer-associated death, with early recognition having an essential function in enhancing patient endurance rates. The research highlights are given below:

- The research goal is to develop a concurrent polyp detection system for endoscopic videos utilizing advanced computer vision techniques to enhance early CRC diagnosis and patient endurance rates.
- The data is gathered from endoscopic video datasets.The data is pre-processed utilizing Contrast-Limited Adaptive Histogram Equalization (CLAHE) to improve image contrast and Histogram of Gradients (HOG) for feature extraction to improve the visibility and detection of polyps.
- The research establishes the AMC-RCN system that combines mask R-CNN for polyp localization and ACFO for hyper-parameter tuning and multi-scale processing.
- The proposed method achieves superior polyp detection accuracy, faster training convergence, and robust segmentation performance,

effectively handling small and irregular polyps in complex endoscopic scenarios.

The AMC-RCN framework significantly improves concurrent polyp recognition in endoscopic videos, demonstrating high clinical applicability and potential for enhancing early CRC diagnosis, ultimately reducing mortality rates.

The remaining research is prepared as follows: Section 2 summarizes the interrelated articles. Section 3 provides the suggested technique. Section 4 demonstrates the research findings. Section 5 gives the discussion and Section 6 summarizes the research's conclusion.

2. Literature review

This section summarizes the traditional approaches and advancements in polyp detection, focusing on recent DL techniques. It highlights the strengths and limitations of current systems using endoscopic video. Table 1 demonstrates the outline of the traditional works on early detection of polyps.

Table 1. Outline of the related polyp detection

Author	Objective	Technique used	Performance metrics	Limitation
Krenzer *et al.*, (2023) [11]	Open-source automated polyp detection system	You Only Look Once (YOLOv5) (adv.), Region-Enhanced Progressive Pooling (REPP) and concurrent-REPP	The REPP achieved higher precision and an F1 score of 90.24	Dataset bias, latency, no clinical trials, over-reliance, and regulatory challenges
Jha *et al.,* (2021) [12]	Automatic recognition and segmentation of polyps	Colonoscopy Segmentation Network (ColonSegNet)	Superior trade-off between accuracy (0.8000), Intersection over Union (IoU) (0.8100), and speed (182.38 Frames Per Second (FPS))	Reproducibility and fair comparisons
Lee *et al.,* (2020) [13]	Automatic polyp detection system	Convolutional Neural Network (CNN) and Long Short-Term Memory (LSTM)	The technique achieved 92.5% accuracy on dataset A, 89.1% on dataset B, and 91.3% on dataset C	Requires improvement in real-time video processing and generalization across diverse populations
Nogueira-Rodríguez *et al*., (2022) [14]	Real-time polyp detection	YOLOv3	The system achieved an F1 score (0.88)	Limitations in detecting flat polyps and small sizes.
Poon *et al.,* (2021) [15]	Colorectal neoplasm localization	AI-Endoscopist (AI-doscopist)	It achieved 96.9% sensitivity in locating polyps	Real-time adaptation
Yu *et al.,* (2022) [16]	Polyp lesion detection	Single Shot MultiBox Detector (SSD) + Instance Tracking Head (ITH)	The model achieves 91.70% mAP and 92.50% accuracy at 66 FPS	Challenges in fine-grained tracking persist
Livovsky *et al.,* (2021) [17]	Detection of elusive polyps	Deep Ensemble Expert-based Polyp detection 2 (DEEP2)	It achieved 97.1% sensitivity, detecting additional polyps missed by endoscopists	Is need further validation
Si *et al.,* (2022) [18]	Improve computational power	YOLOv5-Lite-Prune + EfficientNetLite	The model achieves over 30 FPS with reduced parameters	Despite efficiency improvements,

	in the polyp detection task		and computational complexity	deployment on ultra-low-power devices
Liu *et al*., (2024) [19]	Tiny polyp recognition from endoscopic video	Swin Transformer	enhanced recognition precision by 7%, recall by 7.3%, and average accuracy by 7.5%	Struggles with high computational costs
Wu *et al*., (2021) [20]	Detect gastric cancer in an early stage	CNN	Experts in sensitivity, achieving 92.8% accuracy	False positives and reliance on retrospective data
Li *et al*., (2023) [21]	Real-time polyp detection	Enhanced LSTM (E-LSTM)	Results showed higher accuracy than standard LSTM	Computational complexity and reliance on large labeled datasets
He *et al*., (2023) [22]	Nasopharyngeal carcinoma (NPC) detection	YOLO	The model achieved 0.977 precision and 52.9 FPS	Reduced performance on external data
Fitting *et al.,* (2022) [23]	Preclinical assessment of CADe systems in colonoscopy	YOLOv5	Achieved higher sensitivity (54% vs. 48.1%) and faster FDT (217ms vs. 1050ms)	Dataset diversity and real-world validation.
Sharma *et al.,* (2023) [24]	Automate the extraction of key frames from colonoscopy videos to improve CRC prediction.	YOLO-based Colorectal Lesion Detection (YcOLOn)	The evaluation showed a 96.3% reduction in frames and improved detection performance.	Reliance on specific datasets and the need for long-term validation
Lau *et al*., (2024) [25]	Adenoma Detection Rate (ADR) among endoscopists-in-training	Endoscopy AI Device (ENDO-AID)	Significantly increased overall ADR (57.5% vs 44.5%)	lack of image enhancement
Fu *et al.,* (2024) [26]	polyp detection during endoscopy	Dual-Pyramid and Dual-Modality Polyp Network (D2polyp-Net)	Experiments showed superior accuracy	real-time clinical deployment

Existing polyp detection approaches confront issues such as dataset bias, computational complexity, real-time processing, and generalization across heterogeneous populations. Many rely on historical data, lack clinical validation, and have difficulty recognizing tiny and flat polyps. Furthermore, significant computing costs and deployment constraints impede real-time adaption and large-scale clinical implementation.

3. Methodology

The data is gathered from the polypGen video sequence dataset. The data is preprocessed using CLAHE to improve image contrast and HOG for feature extraction to remove the edge patterns. The AMC-RCN detects polyps in endoscopic videos in real time using Mask R-CNN and ACFO. It improves segmentation accuracy with RPN that adapts convolutional filters and optimizes borders with ACFO. Figure 1 shows the methodological flow.

3.1 Data set

The data is gathered from the PolypGen Video Sequence dataset from Kaggle [27]. The dataset includes 1,537 images, 2,225 video series, and 4,275 negative outlines. It is a collection of mixed residents, endoscopic structures, and specialist comments from six medical centers. The video data is converted into image frames for better polyp detection.

3.2 Data preprocessing

The gathered data images are contrast-enhanced using CLAHE. The CLAHE approach controls a tiny portion of the image known as a tile.

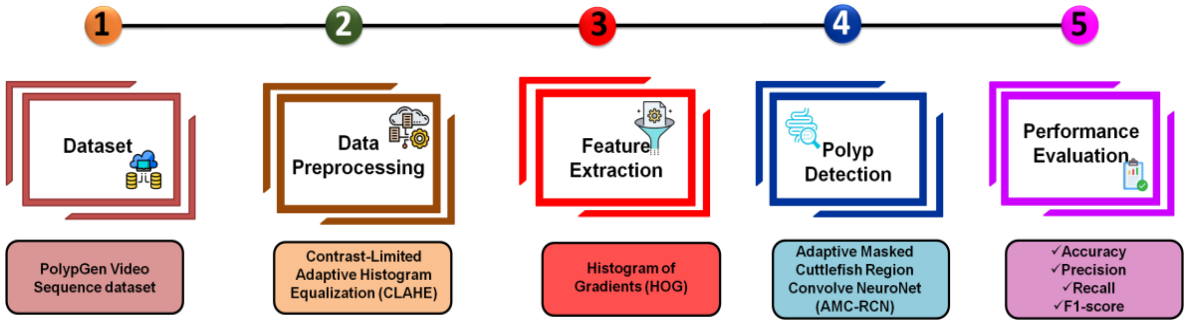

Figure 1. Methodological flow.

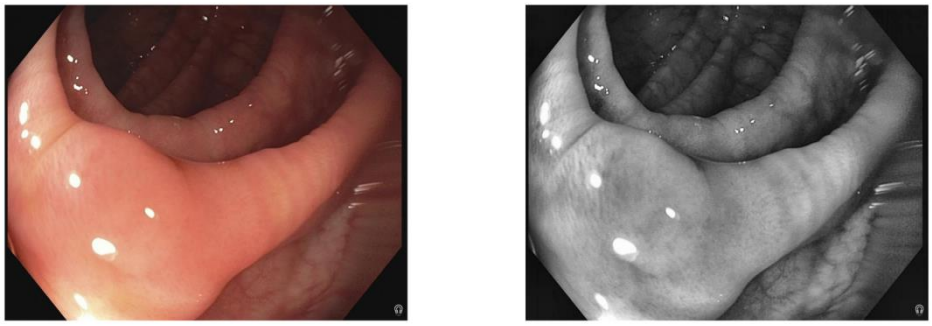

a) Original image b) Processed image

Figure 2. CLAHE outcomea) original image and b) preprocessed image.

Each tile's contrast is corrected to ensure that the histogram created matches the prescribed profile. The closest tiles are linked via bilinear exclamation. This procedure ensures that the merged tiles seem smooth. The approach is described as Equation (1).

$$\beta = \frac{N}{M}\left(1 + \frac{\alpha}{100}\left(t_{max} - 1\right)\right) \quad (1)$$

β denotes the border significance (clip limit), changeable N is the region dimension, M denotes the grey-level assessment, and $\alpha$is the cut-off feature, which adds a histogram border with a rate between 1 and 100. $t_{max}$is the highest permitted angle. This optimizes local contrast, reduces over-amplification, improves feature extraction, normalizes illumination, increases model performance, maintains textural features, and assures robustness. Figure 2 shows the preprocessing outcome: a) original image and b) preprocessed image.

3.3 Feature extraction

The contrast-enhanced data features are extracted using HOG. In this process, the images are first divided into defined parts or cells, which are then grouped into blocks. Equations (2) and (3) are used within each block to calculate the gradient's magnitude and direction.

$$\mathrm{h} = \sqrt{\mathrm{h_w(v,u)^2 + h_z(v,u)^2}} \quad (2)$$

$$\theta = \arctan\frac{\mathrm{h_w(v,u)}}{\mathrm{h_z(v,u)}} \quad (3)$$

$h_w(v,u)$is the incline in the straightway at pixel, $h_z(v,u)$ is the incline in the upright way at pixel, and h indicates a strong edge. $Arctan$Computes the angle of the ascent vector, and $\theta$is the track of the significant intensity change. A feature vector is formed from the distribution of unsigned gradient orientations inside each cell of the block, weighted by their magnitudes. The descriptor for every block, represented as $\mathrm{E^{(p)}}$, is created by normalizing and conceding these vectors. The integer of blocks in the image is designated by n where p varies from $1, 2, 3, \ldots, \mathrm{n}$. These building blocks are essential parts of the cancer detection system.

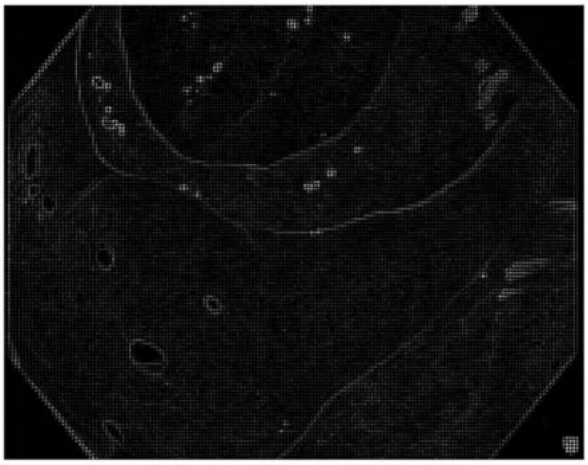

Figure 3. HOG outcome.

The key points matrix, $\mathrm{E^{(i)}} = \mathrm{E^{(p)}}$, is then created by separately extracting each block descriptor, $\mathrm{E^{(p)}}$to creates $\mathrm{E^{(i)}}$ belongs to $\mathrm{E^{(i)}} \in \mathrm{R^{n\times c}}, \mathrm{i} = 1, 2, 3, \ldots, \mathrm{m}$

where i stands for each image sample in the data m for the sum of images and d for the number of elements in the block descriptor. Equation (4) shows us d significance.

$$d = bins \times (CPB)^2 \quad (4)$$

The variable $bins$ represented the quality of gradient orientations, whereas CPB indicates the number of cells per block in this instance. This improves polyp detection by collecting local texture and edge patterns, which are essential for identifying lesions. Figure 3 denotes the outcome of feature extraction.

3.4 Polyp detection using Adaptive Masked Cuttlefish Region Convolve NeuroNet (AMC-RCN)

AMC-RCN detects polyps in endoscopic videos in real time using Mask R-CNN, ACFO, and RCN. It improves segmentation accuracy with RPN that adapts convolutional filters with RCN and optimizes borders with ACFO.

3.4.1 Mask R-CNN

The feature-extracted data is forecasted using mask R-CNN. It is initiated from the faster R-CNN approach. Faster R-CNN creates a quality map from effort images. The Regional Proposal Network (RPN) identifies regions in images that contain objects. The regional proposals are aggregated and estimated among specified classes. During polyp detection, R-CNN uses a two-step method. The initial phase incorporates using the local request system to establish the bounding boxes of the targets (RPN). Utilizing the Region of Interest (ROI)support process determines the mask for all targets in the second phase. In mask R-CNN, the function of the loss value is minimized using Equation (5).

$$K = K_{class} + K_{box} + K_{mask} \quad (5)$$

In faster R-CNN, K_{class} and K_{box} are acknowledged as comparable words. An Equation (6) and (7) defines these terms.

$$K_{class} + K_{box} = \frac{1}{M_{cls}} \sum_j K_{cls}\left(o_j, o_j^*\right) + \frac{1}{M_{box}} \sum_{,} o_j^* M_j^{smooth}\left(s_j, s_j^*\right) \quad (6)$$

$$K_{cls}\left(\left\{\left(o_j, o_j^*\right)\right\}\right) = -o_j^* \log o_j^* - \left(1 - o_j^* \log\left(1 - o_j^*\right)\right) \quad (7)$$

M represents the total number of objects and bounding boxes, o_j is a classification score and the ground truth label o_j^*. $s_j$is the forecasted coordinates and s_j^* is the opinionprecision coordinates. M_j^{smooth} is the smooth loss applied to bounding box regression. The loss of mean neutral cross-entropy, K_{mask}, is determined by Equation (8).

$$K_{mask} = \frac{1}{n^2} \sum_{0 \le j,i \le n} [\, x_{ji} log p x_{ji}^l + \left(1 - x_{ji}\right) \log(1 - x_{ji}^l)] \quad (8)$$

Where, n denotes the dimension of the image, x_{ji} is the ground truth pixel, and px_{ji}^l represents the forecasted probability of a polyp. Mask R-CNN improves polyp detection by creating precise bounding boxes and pixel-wise segmentation masks, resulting in accurate localization, enhanced feature extraction, and strong performance in real-time detection.

3.4.2 Adaptive Cuttlefish Optimization (CFO)

The ACFO algorithm is used to optimize parameters $K_{class}, K_{box}, and\ K_{mask}$ for more accurate validity evaluation. ACFO is a meta-heuristic bio-inspired optimization algorithm to identify the optimal subset of characteristics. This simulates the cuttlefish's color-enhancing habit. The ACFO algorithm relies on reflection and visibility to discover optimal solutions. Reflection mimics light reflection, while visibility mimics similar patterns. The ACFO technique ranks dataset features according to their location before selecting the best subset using Principal Component Analysis (PCA) components. A ranked array (r_A) is defined, and an algorithm creates a population (o) of 35 solutions, each with between 3 and 45 features. Each solution (o_j) is separated into two subsets: unselected and selected, to avoid overlap. The best solutions are saved in $Bw_{bS}$and bS, with bS always having 10% fewer features than Bw_{bS}. The search approach then refines feature selection using reflection (Q) and visibility (U) stages, which include six scenarios.

3.4.2.1 Scenario 1 and 2

The method sorts the inhabitants (o) in a downward array based on robustness scores. After that, a nS_j is created from all resolution o_j, where $j = 1,2,3, \ldots . l$ and (l) is anaccidentally produced numeral digit among (0 and M/2). Equations (9-11) modify the ACFO algorithm's (Q) and (U) operations for these two scenarios.

$$nS_j = Q_j \cup U_j \quad (9)$$

$$Q_j = rS\ [Q] \subset o_j.sF \quad (10)$$

$$U_j = rS\ [U] \subset o_j.uF \quad (11)$$

rS is the random subset, and uF is the unselected features. These subsets are produced randomly from both unselected and chosen features. (Q) and (U)are computed as follows in Equations (12 and 13).

$$Q = rand\ \left(0, o_j.Size_{\ selected}\right) \quad (12)$$

$$U = o_j.Size_{\ selected} - Q \quad (13)$$

3.4.2.2 Scenario 3 and 4

To simulate these instances, Equations (14- 16) are used to create a new subset from the best subset. The feature $s$is treated as a numeral generated by the user. The t $s$value is situated at 5 based on extensive investigational testing. The following stage involves calculating fitness values for each new subset. The last phase is to substitute the best subset. Combine selected features into a new subset if its fitness value exceeds that of the best subset.

$$Q = bS.SF\ [Q] \quad (14)$$

$$U = bS.uF\ [Q] \quad (15)$$

$$nS = Q \cup U \quad ((16)$$

Q represents the feature index to remove from the selected feature, whereas U represents the feature index to choose from the unselected feature. Q and U is calculated using Equations (17 and 18).

$$Q = rand\ (0, bS.Size_{\ selected}) \quad (17)$$

$$U = bS.Size_{\ selected} - Q \quad (18)$$

3.4.2.3 Scenario 5

To simulate this instance, start by generating a new subset from $Bw_{bS}n$ times using Equations (19-21). The variable n represents a user-generated integer number. This method sets the $n$value to 10 based on extensive experimental testing. The following stage involves calculating fitness values for each new subset. The final step is to replace the best subset. Combine selected features into a new subset (nS) if its fitness value exceeds that of the best subset (bS).

$$Q = Bw_{bS}.SF \quad (19)$$

$$U = bS.uF\ [j] \quad (20)$$

$$nS = Q - U \quad (21)$$

$j$is the element value that must be removed from the Bw_{bS}, SF.

3.4.2.4 Scenario 6

The above scenario produces $M - L$ random positions, with L characterizing a formerly shaped random integer from the initial and second scenarios. If the robustness value of the recently twisted solution surpasses that of the Bw_{bS}, it is utilized as a substitute. It enhances feature selection by simulating adaptive color-changing activities, improving segmentation margins, optimizing hyper-parameters, and ensuring accurate recognition of small and irregular polyps in real-time endoscopic video analysis.

The AMC-RCN enhances polyp detection by incorporating Mask R-CNN and ACFO. This method improves segmentation accuracy by refining boundaries and optimizing feature selection. ACFO dynamically modifies hyper-parameters, resulting in more competent training and speedier convergence. The Mask R-CNNconstituent tailors convolutional filters to experiential polyp regions, resulting in enhanced feature extraction and multi-scale processing. AMC-RCN efficiently supervises tiny and irregular polyps under complex endoscopic surroundings, making it suitable for concurrent scientific applications. Its accurate detection potential aids in early identification, considerably reducing CRC hazard and improving patient outcomes. Algorithm 1 shows the working procedure of suggested AMC-RCN model.

Algorithm 1. Adaptive Masked Cuttlefish Region Convolve NeuroNet (AMC-RCN) method

Start

Step 1*: initialize the parameters for mask-R-CNN and CFO*

Step 2*: Mask R-CNN*

Initialize Mask R-CNN model

Load input images

For each image:

Generate feature maps using CNN

Identify region proposals using RPN

Extract object features using ROI Align

Predict bounding boxes and segmentation masks

Store extracted features

Step 3*: Feature Selection using CFO*

Initialize the population with N solutions (each solution is a subset of features)

Define ranked feature list from PCA components

Set constraints: min and max number of features

Repeat until the stopping condition is met:

For each solution:

Divide into selected and unselected subsets

Apply reflection (Q) and visibility (U) to update subsets

Evaluate the fitness of new subsets

Update the best solution if the improvement is found

Return optimized feature subset

Step 4*: Classification using Optimized Features*

Train classifier using selected features

Evaluate model performance on test data

Return final classification results

End

4. Results

The method is performed in Windows 10 (64-bit), Intel(R) Core(TM) i5-3320M CPU @ 2.60GHz and

8GB RAM. A minimum of 200GB storage in the C Drive is required for dataset management and model training. The solution employs Python 3.13.1, Tensor Flow, Keras, and Scikit-Learn for DL-based polyp detection, ensuring real-time processing, precise segmentation, and dependable model performance in endoscopic video analysis. The method's performance is evaluated utilizing different metrics, including accuracy, F1-score, recall, and precision. The method is compared with traditional methods like ASODE [29], YOLOv8 [30] and SIFT [28].

4.1 Evaluation phase

This section evaluated the suggested models performance using Receiver Operating Characteristic (ROC).

4.1.1 ROC

It is utilized to compute a method's capacity to recognize and design the True Positive (TP) Rate about the False Positive (FP) Rate at various entries. This curve employs an Area Under Curve (AUC) rate to evaluate the AMC-RCN system's potential to distinguish polyps. Figure 4 displays the predictable AUC value.

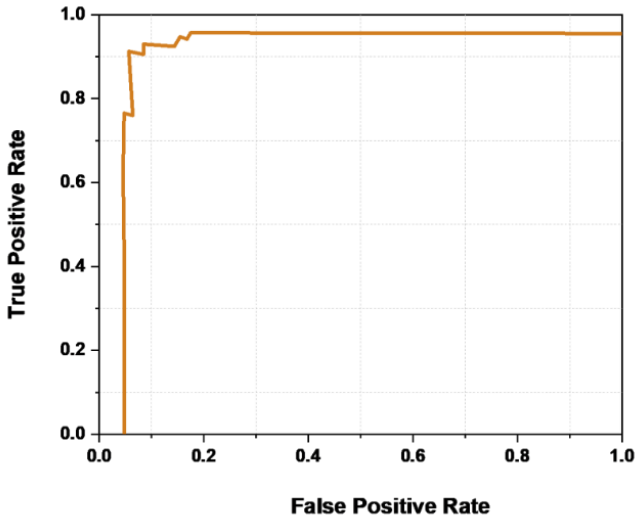

Figure 4. Graphical representation of AUC for proposed AMC-RCN method.

The ROC curve represents how well the AMC-RCN method works in detecting polyps by categorizing troubles at diverse thresholds. The method reveals outstanding forecast accuracy, effectively reducing FP, with a curve in the upper left corner and an AUC of 0.98. This important increase in reduced FP rates demonstrates the algorithm's strong decision-making abilities and verifies the suggested optimization framework's exactness and reliability in recognizing system flaws.

4.2 Comparison Analysis

A comparative analysis is conducted against traditional methods such as SIFT [28], ASODE [29] and YOLOv8 [30], to assess the efficiency of the ACM-RCN system for real-time polyp detection. It is evaluated using various metrics like F1-Score, accuracy, recall, and precision.

4.2.1 Accuracy

It is defined as the fraction of all accurate forecasts produced by the model. Figure 5 and Table 2 display the accuracy results for the recommended and existing methods. Accuracy is calculated by the given Equation (22).

$$Acc = \frac{True_{positive}+True_{negative}}{True_{positive}+True_{negative}+False_{positive}+False_{negative}} \quad (22)$$

Table 2. Numerical findings of accuracy rates

Method	Accuracy (%)
SIFT [28]	96.7
ASODE [29]	92.31
YOLOv8 [30]	92.24
AMC-RCN [Proposed]	98.02

In polyp detection, the suggested AMC-RCN model achieves the maximum accuracy of 98.02%, outperforming the SIFT model (96.7%), YOLOv8 (92.24%), and the ASODE model (92.31%). The AMC-RCN's excellent accuracy suggests that it is used in real-time, improving clinical results for early CRC diagnosis and polyp detection in colonoscopies.

4.2.2 Precision

Precision is definite as the relation of exactly forecasted optimistic occurrences to all cases the algorithm projected as positive. Comparative precision results are displayed in Figure 6 and Table 3. Precision is computed using Equation (23).

$$Pre = \frac{True_{positive}}{True_{positive}+False_{positive}} \quad (23)$$

Table 3. Numerical outcome of precision rates

Method	Precision (%)
SIFT [28]	88.4
ASODE [29]	85.71
YOLOv8 [30]	96.02
AMC-RCN [Proposed]	97.91

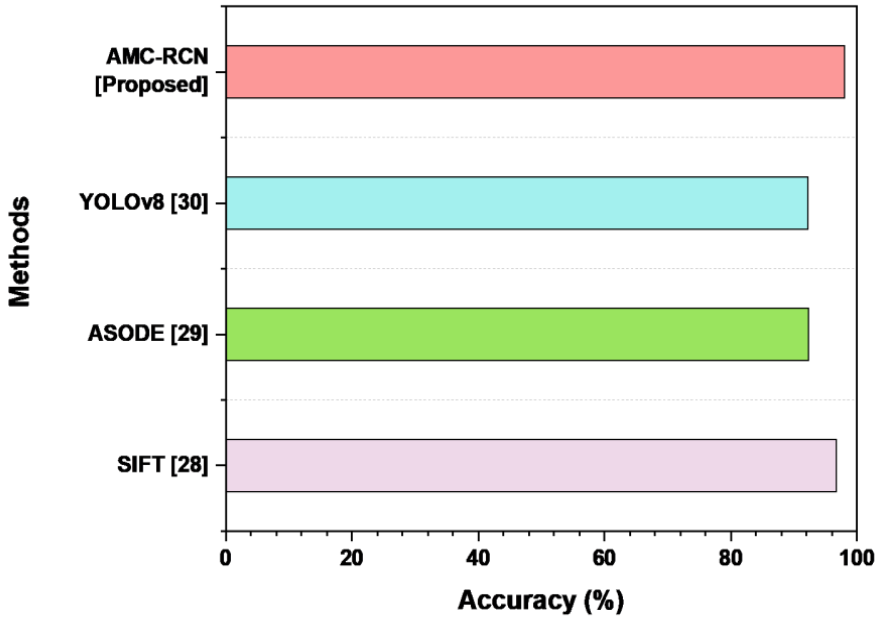

Figure 5. Comparison accuracy result of proposed and prior studies.

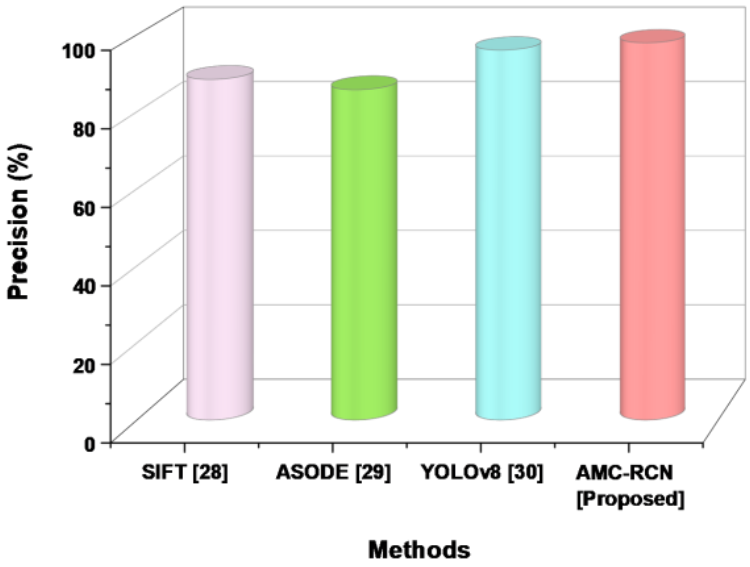

Figure 6. Comparison result of proposed AMC-RCN and prior studies.

The most accurate model is the AMC-RCN model, which achieved 97.91% precision, greatly surpassing the ASODE model (85.71%), SIFT (88.4%), and the YOLOv8 (96.02%). The exceptional accuracy of the AMC-RCN demonstrates its capacity to lower FP and is an essential component for concurrent medical purposes.

4.2.3 Recall

The capacity of the system to properly recognize pertinent examples of the practices from among all of the real instances that are available. The memory of the identification of the model practices is shown in Figure 7 and Table 4. Recall is calculated using Equation (24).

$$Recall = \frac{True_{positive}}{True_{positive}+False_{negative}} \quad (24)$$

Table 4. Recall values for proposed AMC-RCN and conventional strategies

Method	Recall (%)
SIFT [28]	83.2
ASODE [29]	86.42
YOLOv8 [30]	95.90
AMC-RCN [Proposed]	97.07

The AMC-RCN model outperforms the YOLOv8 model (95.90%), SIFT (83.2%), and the ASODE model (86.42%), exhibiting the maximum recall at 97.07%.

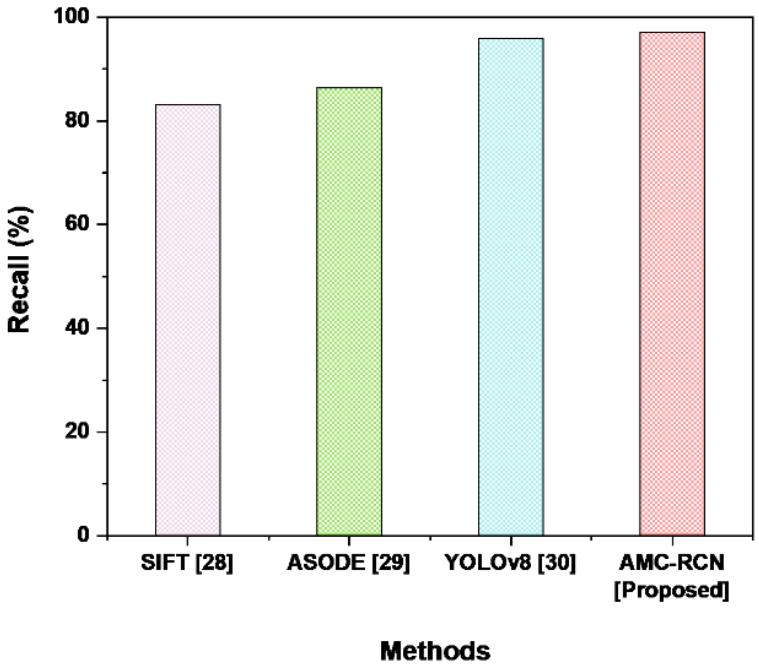

Figure 7. Prediction outcome of proposed AMC-RCN model and conventional strategies.

The improved recall performance implies that AMC-RCN is especially well-suited for uses like medical diagnostics to detect a polyp and has direct repercussions.

4.2.4 F1-score

It is used to assess test success in binary identification. The harmonic means of recall and precision are used to calculate it. Figure 8 and Table 5 denote the F1 score rates for the present and suggested methods. It is evaluated by Equation (25).

$$F1 = 2 \times \frac{precision \times recall}{precision + recall} \quad (25)$$

Table 5. Analyzing F1-Score values for Proposed and existing strategies

Method	F1-score (%)
SIFT [28]	85.6
ASODE [29]	86.06
YOLOv8 [30]	95.96
AMC-RCN [Proposed]	96.97

The AMC-RCN method performs better at balancing precision and recall for polyp identification, achieving the greatest F1-score of 96.97%. The AMC-RCN surpasses the ASODE model (86.06%), SIFT (85.7%), and the YOLOv8 (95.96%), demonstrating its ability to handle a variety of polyp features and produce more dependable detection results. This notable increase in the F1 score highlights the AMC-RCN's ability to offer reliable and accurate detection. The comparison analysis clearly demonstrates that the AMC-RCN model outperforms previous methodologies in terms of recognition accuracy, segmentation precision, and adaptability to complex and irregular polyp shapes. Unlike conventional approaches, AMC-RCN efficiently handles a wide range of polyp shapes while ensuring reliable identification. Its sophisticated architecture makes it ideal for real-time clinical use, providing faster and more precise results during endoscopic operations while increasing diagnostic reliability.

5. Discussion

CRC was the most general cancers in the globe, although its incidence and mortality rates have dropped significantly by around 51% and 32%, correspondingly due to advances in routine transmission and adenomatous polyp deletion. The finding and recognition of endoscopic observation technologies, together with the development of computer vision and DL systems, have changed gastrointestinal diagnostics by enabling concurrent detection and precise segmentation of cancerous injuries. These improvements facilitate besieged biopsies and the effectual removal of precancerous polyps, eliminating the requirement for preventable models and medical waste. Concurrent polyp detection in endoscopic recordings was significant for early CRC diagnosis, which enhanced patient endurance rates by allowing for imperative medical interferences. Automated recognition enhanced accuracy and reliability while lowering the likelihood of human error in polyp recognition.

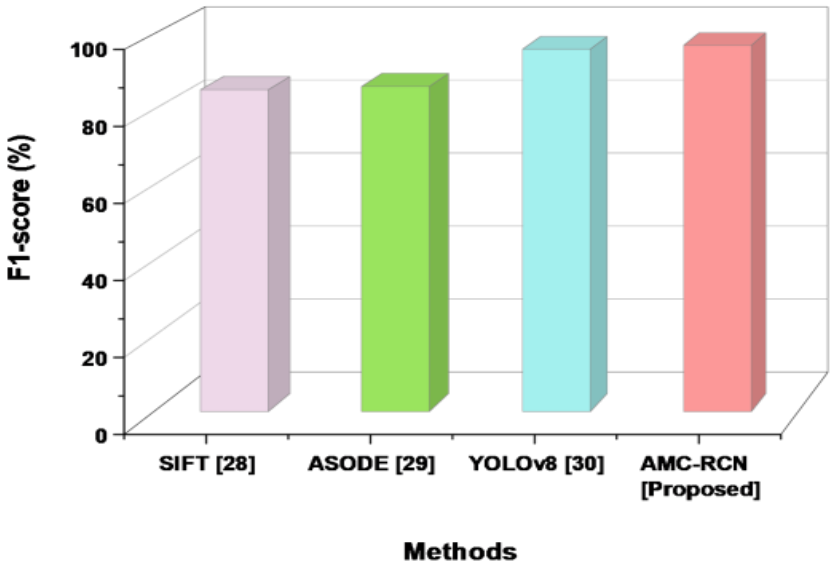

Figure 8. Graphical representation of F1-Score.

It also enlarged medical effectiveness by sustaining endoscopists in concurrent, allowing for quicker decision-making during actions. Sophisticated recognition frameworks enhanced segmentation and feature extraction even under tricky imaging conditions, increasing diagnostic consistency. Furthermore, concurrent technologies support minimally persistent screening, minimizing unnecessary biopsies and improving patient care while critical healthcare expenditures. The objective of this research was to generate an enhanced technique for concurrent polyp detection in endoscopic videos that ensures precise segmentation and capable feature selection. Despite remarkable improvements in computerized polyp recognition employing sophisticated DL methods includes YOLOv5, ColonSegNet, CNN-LSTM, Swin Transformer, and D2polyp-Net, important research gaps persist. Several studies have informed high precision recital. However, limitations like dataset bias [11], reproducibility issues [12], a need of scientific validation [17], and generalization concerns across various populations [13] remain. Additionally, high processing rates [19], concurrent alteration problems [15], and poor performance on low-resource systems [18] hinder extensive use. Previous systems often rely on labelled datasets and lack interpretability, reducing medical belief. As a result, there was an important gap in embryonic insubstantial, capable, concurrent, and clinically validated polyp recognition methods that ensure fairness, scalability, and flexibility across varied settings for better analytical accuracy and realistic exploitation in endoscopy workflows. The AMC-RCN was compared to traditional systems, including SIFT [28], ASODE [29], and YOLOv8 [30]. SIFT [28], a well-known keypoint-based feature extraction technique, falls short in medical imaging situations such as endoscopic recordings, where polyps frequently have low contrast, irregular forms, and subtle textural variations. It fails to capture the contextual and spatial interactions necessary for accurate polyp detection. ASODE [29], an advanced optimization method, improves feature selection capabilities, but its computationally demanding operations make it unsuitable for real-time applications. Furthermore, it does not include pixel-level segmentation, which was necessary for precisely identifying polyp borders. YOLOv8 [30], an advanced DL-based object recognition method, was particularly capable and provided concurrent recognition capabilities. However, YOLOv8 [30] was mainly consscerned with bounding box detection and required the fine-grained segmentation potential necessary to accurately perceive tiny or flat polyps with confusing boundaries. Additionally, YOLOv8 [30] misclassify or totally ignore polyps that required major attributes, resulting in FN. The AMC-RCN method resolves these constraints by utilizing ACFO, which suggested cuttlefish adaptive color inflection activity, dynamically tuning hyper-parameters and alternative the most pertinent characteristics from endoscopic images [31]. This enables the system to process segmentation boundaries efficiently while decreasing preventable estimates, making it ideal for concurrent medical relevance. The Mask R-CNN constituent helps by generating bounding boxes and pixel-wise segmentation masks, which bridges the gap among recognition and precise localization. Furthermore, AMC-RCN employed multi-scale processing techniques to precisely spot both tiny and big polyps, despite of their position or outline. Unlike traditional methods, the suggested system was capably deal with rough structures, overlapping tissues, and erratic lighting circumstances. This full incorporation not only improved recognition performance, but it also speeds up training convergence and increased clinical reliability. Overall, the AMC-RCN framework

outperformed traditional systems by addressing key restrictions with intelligent optimization, adaptive filtering, and accurate segmentation capabilities, making it a capable device for improving CRC screening and early intervention tactics. The AMC-RCN system has substantial therapeutic applications because it allows for the real-time and extremely precise detection of polyps in endoscopic recordings [32]. Its combination of segmentation precision and adaptive feature optimization ensures early detection of malignant precursors, which improved patient outcomes and lowers CRC mortality [33]. The model's capacity to deal with small, irregular polyps and swiftly process video frames makes it perfect for use in real-time clinical settings [34]. This not only decreased the workload for gastroenterologists, but it also eliminated human error, improved diagnostic reliability, and enables speedier clinical decision-making during endoscopic examinations. AMC-RCN marks a substantial step forward in the field of computer-aided colonoscopy by combining biologically inspired optimization with cutting-edge DL architecture. Its comprehensive technique, which combined detection, segmentation, and adaptive optimization, solves the complex issues of polyp diagnosis in real-time clinical settings. The AMC-RCN architecture outperformed traditional approaches, providing a highly scalable, interpretable, and clinically robust solution that improved CRC screening and paves the path for future intelligent endoscope systems.

6. Conclusion

Polyp detection in endoscopic videos improved early CRC analysis and endurance rates with the reasonable decision-making. It enhanced accuracy, eradicates human error, improves medical efficiency, allows greater segmentation in complicated conditions, assists minimally constant programs, and saves healthcare outlays. The purpose of this research was to create an enhanced framework for concurrent polyp recognition in endoscopic videos, with precise segmentation and capable feature selection to support in early CRC detection. The findings showed that AMC-RCN outperformed standard approaches, attaining higher precision (97.91%), recall (97.07%), accuracy (98.02%), F1-score (96.97%), and more robust handling of tiny and irregular polyps in complex endoscopic settings. However, the model has some disadvantages, such as high computational needs for real-time processing and potential susceptibility to variations in endoscopic imaging parameters. Future research concentrates on increasing computing efficiency, integrating lightweight architectures for real-time deployment, and improving generalization across various datasets to improve clinical applications. Subsequent to the optimization of the ACFO-operated hypermeter, it guarantees superior recognition and rapid convergence relative to conventional approaches by using CLAHE for contrast enhancement and HOG for optimization. The real-time architecture offers substantial advantages for clinical distribution, aiding gastroenterologists in the early detection of CRC and enhancing patient survival rates. Future study should concentrate on enhancing computational efficiency in endoscopic systems for practical applications and broaden validation across diverse datasets to improve generalizability. With further refinement, AMC-RCN prevention has the potential to evolve into a significant AI-assisted tool for CRC screening, ultimately reducing the worldwide burden of CRC.

References

[1] I. Rebollo, N. Wolpert, & C. Tallon-Baudry, Brain–stomach coupling: Anatomy, functions, and future avenues of research. *Current Opinion in Biomedical Engineering*, 18, (2021) 100270. https://doi.org/10.1016/j.cobme.2021.100270

[2] S. Venugopal, A. Ramaiah, V. S. Panda, S. Ambikapathy, A., & A. MB, Sustainable augmented framework using smart sensors with ATM inspired 5G technologies for enterprise networks. *International Journal of Information Technology*, (2024) 1-8. https://doi.org/10.1007/s41870-024-02013-7

[3] R. L. Siegel, K. D. Miller, N. S. Wagle and A. Jemal, Cancer statistics, 2023. *CA: a cancer journal for clinicians*, 73(1), (2023) 17-48. https://doi.org/10.3322/caac.21763

[4] M. Pinheiro, D. N. Moreira, & M. Ghidini, Colon and rectal cancer: An emergent public health problem. *World Journal of Gastroenterology*, 30(7), (2024) 644. https://doi.org/10.3748/wjg.v30.i7.644

[5] J. Lewis, Y. J. Cha, & J. Kim, Dual encoder–decoder-based deep polyp segmentation network for colonoscopy images. *Scientific Reports*, 13(1), (2023) 1183. https://doi.org/10.1038/s41598-023-28530-2

[6] A. O. Ige, N. K. Tomar, F. O. Aranuwa, O. Oriola, A. O. Akingbesote, M. H. M. Noor, ... & B. S. Aribisala, Convsegnet: automated polyp segmentation from colonoscopy using context feature refinement with multiple convolutional kernel sizes. *IEEE Access*, 11, (2023) 16142-16155. https://doi.org/10.1109/ACCESS.2023.3244789

[7] P. Sasmal, V. Sharma, A. J. Prakash, M. K. Bhuyan, K. K. Patro, N. A. Samee, ... & P. Pławiak, Semi-supervised generative adversarial networks for improved colorectal polyp classification using histopathological images. *Information Sciences*, 658, (2024) 120033. https://doi.org/10.1016/j.ins.2023.120033

[8] L. Xu, X. He, J. Zhou, J. Zhang, X. Mao, G. Ye, ... & C. Yu, Artificial intelligence-assisted colonoscopy: a prospective, multicenter,

randomized controlled trial of polyp detection. *Cancer medicine*, 10(20), (2021) 7184-7193. https://doi.org/10.1002/cam4.4261

[9] W. Jiang, L. Xin, S. Zhu, Z. Liu, J. Wu, F. Ji, C. Yu and Z. Shen, Risk factors related to polyp miss rate of short-term repeated colonoscopy. *Digestive diseases and sciences*, 68(5), (2023) 2040-2049. https://doi.org/10.1007/s10620-023-07848-x

[10] Z. F. Khan, M. Ramzan, M. Raza, M. A. Khan, A. Alasiry, M. Marzougui and J. Shin, Real-time polyp Detection from Endoscopic Images using YOLOv8 with YOLO-Score Metrics for Enhanced Suitability Assessment. *IEEE Access*, (2024). https://doi.org/10.1109/ACCESS.2024.3505619

[11] A. Krenzer, M. Banck, K. Makowski, A. Hekalo, D. Fitting, J. Troya, B. Sudarevic, W. G. Zoller, A. Hann and F. Puppe, A real-time polyp-detection system with clinical application in colonoscopy using deep convolutional neural networks. *Journal of Imaging*, 9(2), (2023) 26. https://doi.org/10.3390/jimaging9020026

[12] D. Jha, S. Ali, N. K. Tomar, H. D. Johansen, D. Johansen, J. Rittscher, M. A. Riegler and P. Halvorsen, Real-time polyp detection, localization, and segmentation in colonoscopy using deep learning. *Ieee Access*, 9, (2021) 40496-40510. https://doi.org/10.1109/ACCESS.2021.3063716

[13] J. Y. Lee, J. Jeong, E. M. Song, C. Ha, H. J. Lee, J. E. Koo, D. H. Yang, N. Kim and J. S. Byeon, Real-time detection of colon polyps during colonoscopy using deep learning: systematic validation with four independent datasets. *Scientific reports*, 10(1), (2020) 8379. https://doi.org/10.1038/s41598-020-65387-1

[14] A. Nogueira-Rodríguez, R. Domínguez-Carbajales, F. Campos-Tato, J. Herrero, M. Puga, D. Remedios, L. Rivas, E. Sánchez, A. Iglesias, J. Cubiella and F. Fdez-Riverola, Real-time polyp detection model using convolutional neural networks. *Neural Computing and Applications*, 34(13), (2022) 10375-10396. https://doi.org/10.1007/s00521-021-06496-4

[15] C. C. Poon, Y. Jiang, R. Zhang, W. W. Lo, M. S. Cheung, R. Yu, Y. Zheng, J. C. Wong, Q. Liu, S. H. Wong and T. W. Mak, AI-endoscopist: a real-time deep-learning-based algorithm for localizing polyps in colonoscopy videos with edge computing devices. *NPJ digital medicine*, 3(1), (2020) 73. https://doi.org/10.1038/s41746-020-0281-z

[16] T. Yu, N. Lin, X. Zhang, Y. Pan, H. Hu, W. Zheng, J. Liu, W. Hu, H. Duan and J. Si, An end-to-end tracking method for polyp detectors in colonoscopy videos. *Artificial intelligence in medicine*, 131, (2022) 102363. https://doi.org/10.1016/j.artmed.2022.102363

[17] D. M. Livovsky, D. Veikherman, T. Golany, A. Aides, V. Dashinsky, N. Rabani, D. B. Shimol, Y. Blau, L. Katzir, I. Shimshoni and Y. Liu, Detection of elusive polyps using a large-scale artificial intelligence system (with videos). *Gastrointestinal Endoscopy*, 94(6), (2021) 1099-1109. https://doi.org/10.1016/j.gie.2021.06.021

[18] B. Si, C. Pang, Z. Wang, P. Jiang and G. Yan, Real-Time Lightweight Convolutional Neural Network for Polyp Detection in Endoscope Images. *Journal of Shanghai Jiaotong University (Science)*, (2023) 1-14. https://doi.org/10.1007/s12204-023-2671-2

[19] E. Liu, B. He, D. Zhu, Y. Chen and Z. Xu, Tiny polyp detection from endoscopic video frames using vision transformers. *Pattern Analysis and Applications*, 27(2), (2024) 38. https://doi.org/10.1007/s10044-024-01254-3

[20] L. Wu, M. Xu, X. Jiang, X. He, H. Zhang, Y. Ai, Q. Tong, P. Lv, B. Lu, M. Guo and M. Huang, Real-time artificial intelligence for detecting focal lesions and diagnosing neoplasms of the stomach by white-light endoscopy (with videos). *Gastrointestinal Endoscopy*, 95(2), (2022) 269-280. https://doi.org/10.1016/j.gie.2021.09.017

[21] J. W. Li, T. Chia, K. M. Fock, K. D. W. Chong, Y. J. Wong and T. L. Ang, Artificial intelligence and polyp detection in colonoscopy: use of a single neural network to achieve rapid polyp localization for clinical use. *Journal of Gastroenterology and Hepatology*, 36(12), (2021) 3298-3307. https://doi.org/10.1111/jgh.15642

[22] Z. He, K. Zhang, N. Zhao, Y. Wang, W. Hou, Q. Meng, C. Li, J. Chen and J. Li, Deep learning for real-time detection of nasopharyngeal carcinoma during nasopharyngeal endoscopy. *Science*, 26(10), (2023). https://doi.org/10.1016/j.isci.2023.107463

[23] D. Fitting, A. Krenzer, J. Troya, M. Banck, B. Sudarevic, M. Brand, W. Böck, W. G. Zoller, T. Rösch, F. Puppe and A. Meining, A video-based benchmark data set (ENDOTEST) to evaluate computer-aided polyp detection systems. *Scandinavian Journal of Gastroenterology*, 57(11), (2022) 1397-1403. https://doi.org/10.1080/00365521.2022.2085059

[24] V. Sharma, P. Sasmal, M. K. Bhuyan, P. K. Das, Y. Iwahori and K. Kasugai, A multi-scale attention framework for automated polyp localization and keyframe extraction from colonoscopy videos. *IEEE Transactions on Automation Science and Engineering*, (2023). https://doi.org/10.1109/TASE.2023.3315518

[25] L. H. Lau, J. C. Ho, J. C. Lai, A. H. Ho, C. W. Wu, V. W. Lo, C. M. Lai, M. W. Scheppach, F. Sia, K. H. Ho and X. Xiao, Effect of real-time computer-aided polyp detection system (ENDO-AID) on adenoma detection in endoscopists-in-training: a randomized trial. *Clinical Gastroenterology and*

Hepatology, 22(3), (2024) 630-641. https://doi.org/10.1016/j.cgh.2023.10.019

[26] J. Fu, Y. Gao, P. Zhou, Y. Huang, J. Jiao, S. Lin, Y. Wang and Y. Guo, D2polyp-Net: A cross-modal space-guided network for real-time colorectal polyp detection and diagnosis. *Biomedical Signal Processing and Control*, 91, (2024) 105934. https://doi.org/10.1016/j.bspc.2023.105934

[27] PolypGen video sequence. (2023, October 1). *Kaggle*. https://www.kaggle.com/datasets/debeshjha1/polypgen-video-sequence

[28] J. Xu, Y. Kuai, Q. Chen, X. Wang, Y. Zhao and B. Sun, Spatio-Temporal Feature Transformation Based Polyp Recognition for Automatic Detection: Higher Accuracy than Novice Endoscopists in Colorectal Polyp Detection and Diagnosis. *Digestive Diseases and Sciences*, 69(3), (2024) 911-921. https://doi.org/10.1007/s10620-024-08277-0

[29] L. Zhao, N. Wang, X. Zhu, Z. Wu, A. Shen, L. Zhang, R. Wang, D. Wang and S. Zhang, Establishment and validation of an artificial intelligence-based model for real-time detection and classification of colorectal adenoma. *Scientific Reports*, 14(1), (2024) 10750. https://doi.org/10.1038/s41598-024-61342-6

[30] A. Ambikapathy, T. D. Beeta, R. K. Kanna, A. Danquah-Amoah, V. S. Ramya, & U. Mutheeswaran, Biometric Application on Facial Image Recognition Techniques. In *2024 IEEE International Conference on Computing, Power and Communication Technologies (IC2PCT)*, Vol. 5, (2024) 848-851. IEEE. https://doi.org/10.1109/IC2PCT60090.2024.10486608

[31] P. Sunthornwetchapong, K. Hombubpha, K. Tiankanon, S. Aniwan, P. Jakkrawankul, N. Nupairoj, P. Vateekul and R. Rerknimitr, Real-Time Multi-Task Deep Learning Model for Polyp Detection, Characterization, and Size Estimation. *IEEE Access*, (2025). https://doi.org/10.1109/ACCESS.2025.3527720

[32] K. Venkatachalam, A. Devipriya, J. Maniraj, M. Sivaram, & A. Ambikapathy, A Novel Method of motor imagery classification using eeg signal. *Artificial intelligence in medicine*, 103, (2020) 101787. https://doi.org/10.1016/j.artmed.2019.101787

[33] A. Ambikapathy, G. Singh, & P. Tiwari, Smart switching algorithm between IC and PO algorithms for grid-connected PV system. In *Advances in smart grid and renewable energy: Proceedings of ETAEERE-2016*, (2017) 83-92. Singapore: Springer Singapore. https://doi.org/10.1007/978-981-10-4286-7_9

[34] Z. Khan, R. K. Kanna, K. Parthasarathy, S. Vijayaraj, R. Chandrasekaran, & S. Jawla, Intelligent computational ensemble model for predicting cerebral aneurysm using the concept of region localization in multi-section CT angiography. *International Journal of Information Technology*, (2025) 1-7. https://doi.org/10.1007/s41870-024-02292-0

Authors Contribution Statement

T. Swetha Kumari – Conceptulaization, Methodology, Investigation, Validation, Formal Analysis and Writing original draft. R. Vasuki – Supervision, Writing, Review and Editing. Both the authors read and approved the final version of this manuscript.

Funding

The authors declare that no funds, grants or any other support were received during the preparation of this manuscript.

Competing Interests

The authors declare that there are no conflicts of interest regarding the publication of this manuscript.

Data Availability

The data supporting the findings of this study can be obtained from the corresponding author upon reasonable request.

Has this article screened for similarity?

Yes

About the License